

arXiv:cond-mat/9912160v1 [cond-mat.supr-con] 9 Dec 1999

Magnetization Measurements on Single Crystals of Superconducting $\text{Ba}_{0.6}\text{K}_{0.4}\text{BiO}_3$

Donavan Hall
National High Magnetic Field Laboratory
Florida State University
Tallahassee, FL 32306-4005

R. G. Goodrich and C. G. Grenier
Department of Physics and Astronomy
Louisiana State University, Baton Rouge, LA 70803-4001

Pradeep Kumar
Department of Physics
University of Florida, Gainesville, FL 32611-8440

Murali Chaparala
Department of Physics
University of Virginia, Charlottesville, VA 22901

M. L. Norton
Department of Chemistry
Marshall University, Huntington, WV 25755-2520

July 28, 2021

Abstract

Extensive measurements of the magnetization of superconducting single crystal samples of $\text{Ba}_{0.6}\text{K}_{0.4}\text{BiO}_3$ have been made using SQUID and cantilever force magnetometry at temperatures ranging between

1.3 and 350 K and in magnetic fields from near zero to 27 T. Hysteresis curves of magnetization versus field allow a determination of the thermodynamic critical field, the reversibility field, and the upper critical field as a function of temperature. The lower critical field is measured separately and the Ginzburg-Landau parameter is found to be temperature dependent. All critical fields have higher $T = 0$ limits than have been previously noted and none of the temperature dependence of the critical fields follow the expected power laws leading to possible alternate interpretation of the thermodynamic nature of the superconducting transition.

PACS numbers: 74.60.-w, 74.25.Ha, 74.25.Dw, 74.25.Bt

Accepted for publication in *Philosophical Magazine B* on 7 August 1999

1 Introduction

The discovery of high T_c superconductivity in $(\text{La,Ba})_2\text{CuO}_4$ (Bednorz and Müller, 1986) was partly inspired by the bismuthate superconductor, $\text{Ba}(\text{Pb,Bi})\text{O}_3$ (Sleight, Gilson, and Bierstedt, 1975). Subsequent cuprate superconductors command the attention of a great many researchers because of their high T_c s (on the order of 100 K). The discovery of high T_c superconductivity (HTSc) in the bismuthate system $\text{Ba}_{1-x}\text{K}_x\text{BiO}_3$ (BKBO) more than ten years ago (Cava, Batlogg, Krajewski, Farrow, Jr, White, Short, Peck, and Kometani, 1988; Mattheiss, Gyorgy, and Johnson Jr., 1988; Hinks, Dabrowski, Jorgensen, Mitchell, Richards, Pei, and Shi, 1988) with a T_c of 30 K began an equally significant, complementary course of research into the nature of HTSc for the following reasons: (1) it contains no copper, (2) it is an isotropic conductor, (3) it has no evident magnetic ordering off stoichiometry, (4) its superconductivity occurs at the boundary of a metal-insulator transition (a commonality with the cuprates) (Hinks, Dabrowski, Jorgensen, Mitchell, Richards, Pei, and Shi, 1988; Dabrowski, Hinks, Jorgensen, Kalia, Vashishta, Richards, a. Mark, and Mitchell, 1988; Sato, Tajima, Takagi, and Uchida, 1989), (5) normal state resistivity measurements evince other than pure metallic behavior (Dabrowski, Hinks, Jorgensen, Kalia, Vashishta, Richards, a. Mark, and Mitchell, 1988), (6) it has two related compounds: $\text{Ba}_{1-x}\text{Rb}_x\text{BiO}_3$, that has a T_c of ≈ 29 K for $0.28 \leq x \leq 0.44$ (Itti, Tomeno,

Ikeda, Tai, Koshizuka, and Tanaka, 1991), and Ba(Pb, Bi)O_3 , a more conventional superconductor with a T_c of ≈ 12 K (Batlogg, 1984), and (7) both BKBO and Ba(Pb, Bi)O_3 have a comparatively low density of states (low carrier densities), given their high values of T_c .

There have been several previous measurements of the magnetic properties of superconducting $\text{Ba}_{1-x}\text{K}_x\text{BiO}_3$ reported in the literature (Batlogg, Cava, Rupp, Mujsce, Krajewski, Remika, Peck, a. Cooper, and Espinosa, 1988), (Welp, Kwok, Crabtree, Claus, Vandervoort, Dabrowski, Mitchell, Richards, Marx, and Hinks, 1988), (McHenry, Maley, Kwei, and Thompson, 1989), (Grader, Hebard, and Scheenmeyer, 1990), (Huang, Fang, Xue, Hor, Chu, Norton, and Tang, 1991). For $x = 0.4$, single crystal measurements of H_{c1} were made by Grader, Hebard, and Scheenmeyer (1990) using an electrodynamic force balance technique on micron-sized single crystal samples. It was found that the lower critical field values measured on their near perfect single crystals were much higher (250 gauss at 10 K) than the H_{c1} values reported by Batlogg et al. (1988) on powdered samples of similar composition (90 gauss at 10 K). Further measurements of H_{c1} on large single crystals have been done by Huang et al. (1991) who also reported low values of 95 gauss at 5 K. All of these measurements were done on samples of imprecisely known demagnetization factors. For single crystals, in Grader et al. (1990), H_{c1} is found to vary linearly with temperature over the range of temperatures measured (7 - 22 K) whereas in Huang et al. (1991) the H_{c1} versus temperature curve shows a downward curvature as $T = 0$ is approached.

The upper critical field H_{c2} also was reported in Batlogg et al. (1988), and extensive H_{c2} studies of powdered samples of varying composition were done by Welp et al. (1988). In the constant-field, temperature-dependent magnetic measurements done by Batlogg et al. (1988) a linear negative slope of $dH_{c2}/dT = -0.5$ T/K between 20 and 29 K was observed. Constant-field, temperature-dependent resistivity measurements of several potassium concentrations obtained by Welp et al. (1988), show that for $x = 0.4$, a slope of -0.6 T/K fit temperatures well below T_c . A slight, positive curvature of dH_{c2}/dT was found near T_c in all of the samples measured in Welp et al. (1988). Recently, Samuely, Szabo, Jansen, Wyder, Marcus, Baril, and Escribe-Filippini (1996) have used tunneling measurements on low T_c samples ($T_c = 20$ K) to determine H_{c2} as a function of temperature; they find much lower values of H_{c2} than in other measurements.

Several recent measurements of the magnetic properties of $\text{Ba}_{1-x}\text{K}_x\text{BiO}_3$ in Gatalaskaya, Barilo, Shirayev, Szymezak, Szymezak, and Baran (1996)

and Goll, Jansen, and Marcus (1996) and in an earlier paper by McHenry, Maley, Kwei, and Thompson (1989) have focused on the reversibility field as a function of temperature. In their study of flux creep in $\text{Ba}_{0.6}\text{K}_{0.4}\text{BiO}_3$, McHenry et al. (1989) found the reversibility field never to exceed 0.8 T down to 5 K. In samples of nominal composition ($x = 0.34$), Gatal'skaya et al. (1996) find good agreement near T_c using a power law: $H_r \approx (1 - T/T_c)^m$ with $m = 1.45$. For samples having a T_c of 20 K, force magnetometer measurements over a temperature range of 0.4 to 20 K by Goll et al. (1996) show a continual upward curvature of H_r extending to 25 T at 0.4 K. Thus different groups have measured widely different values for H_r on different samples.

We report extensive studies of the magnetization of single crystal samples of $\text{Ba}_{0.6}\text{K}_{0.4}\text{BiO}_3$. Magnetic field dependent hysteresis curves of the magnetization at constant temperature were recorded at temperatures ranging from 1.3 to 32 K in applied fields from zero to 27 T, and the temperature dependence of the magnetization was measured from above room temperature down to below the superconducting transition temperature. From these measurements, we derive several quantities: (1) the complete temperature dependence of the lower critical field H_{c1} , (2) the upper critical field H_{c2} , (3) the reversibility field H_r , and (4) the thermodynamic critical field H_0 . All of these critical fields are determined as a function of temperature. In addition, the temperature dependence of the normal state susceptibility is determined.

These results highlight the unique nature of the properties of BKBO. While the qualitative features of the magnetic properties are quite reasonable, and look much like any other superconductor, in detail, BKBO has a remarkable number of anomalous properties. For example, in a conventional superconductor, both H_{c1} and H_{c2} have the same temperature dependence. Indeed the ratio, H_{c2}/H_{c1} , within logarithmic factors, is the square of the Ginzburg-Landau (GL) parameter, κ , and is temperature independent near T_c . In BKBO, H_{c1} and H_{c2} have different temperature dependences, leading to a temperature dependent (and divergent at T_c) κ . The thermodynamic critical field $H_0 \propto (1 - T/T_c)^2$ in contrast to a conventional superconductor where the exponent is one. The specific heat discontinuity at T_c appears to be zero. Likewise, we find the discontinuity in the magnetic susceptibility to be zero. When all of these results are taken together, it has recently been shown Kumar, Hall, and Goodrich (1999) that a new model for the thermodynamic nature of the phase transition from the normal to SC state gives good agreement with the results.

This paper is organized as follows: In section 2 we briefly describe the

sample preparation technique following Norton and Tang Norton and Tang (1991). Section 3 contains a description of measurement techniques in detail. Section 4, divided into five subsections, goes through the results for H_{c1} , H_0 , H_{c2} , H_r and finally the normal state, temperature dependent magnetic susceptibility. Section 5 presents our current understanding of these results, relating them to earlier measurements. We also include a brief discussion of the properties of phase transitions of order > 2 , and how they relate to the results presented here. The paper ends with a summary of our conclusions in section 6.

2 Sample Preparation

The crystals used in this study were grown by scaling up the electrosynthetic method described by Norton and Tang (1991). A typical procedure, briefly listing the essential modifications, is given here. An initial charge of 344 g of KOH (Baker, Reagent Grade) and 41 g Bi_2O_3 (Baker, Analyzed) was melted in a 300 ml PFA transfer container (Berghof / America) using a temperature regulated (Omega) heating mantle (Glas-Col), with stirring, producing a solution saturated with bismuth ions. To this solution, 27 g of $Ba(OH)_2 \cdot 8H_2O$ (Matheson, Reagent) was slowly added, with stirring, under an atmosphere of flowing water saturated nitrogen, an inert cover gas. After the solution clarified, and stabilized at 240 °C, a 2 mm diameter (0.1mm wall thickness) platinum tubing cathode (Goodfellow, 99.95 %), a 3.2 mm diameter bismuth rod reference electrode (ESPI, 5N purity) and a 1 mm diameter silver wire anode (Aesar, 99.9 %) were inserted 1 cm into the solution. A potential of 0.69 V was applied utilizing a potentiostat (BAS model CV 27). Multiple crystals were harvested after 340 hours by extraction of the silver anode with the firmly attached crystals from the molten solution, followed by air cooling. Adhering solidified flux was removed by rinsing with distilled water. The samples were air dried, and the least flawed single crystals displaying cubic morphology were chosen for this study.

The high T_c (> 30 K) found for these crystals suggests that they were very close to the optimal superconducting stoichiometry. Subsequent X-ray analysis showed the 1 mm^3 facets used in these experiments were single perovskite crystals with a mosaic spread of less than 2° .

One of the problems in determining H_{c1} has been the fact that the sample demagnetizing factor is of importance for this measurement. Without

a controlled demagnetizing geometry, flux begins to penetrate the sample at different fields depending on position in the sample. For this reason we produced a single crystal sphere for the H_{c1} measurements. Starting with a crystal of approximately $1.5 \times 1.5 \times 1.5 \text{ mm}^3$ and a T_c of 30 K we ground it into a sphere in an air driven racetrack using a diamond sandpaper abrasive. The resulting sphere had a diameter of 1 mm. After grinding the sphere, it was annealed in O_2 for 24 hours at 400 °C. Laue pictures showed no signs of strain.¹ After this processing the sample used for the H_{c1} measurements had a T_c of approximately 29 K.

3 Measurements

The measurements near T_c reported here were made using a Quantum Design MPMS SQUID magnetometer ($B < 5.5 \text{ T}$). Several precautions must be made in measurements on superconductors near T_c using a measurement system of this type. There are two basic problems. First, the magnetic moment of the sample holder can easily become larger than that of the sample near T_c , and the maximum moment of the sample holder combined with the sample shifts along an axis parallel to the applied field. When this occurs, the output voltage from the SQUID pickup coils is not centered and spurious results in the calculation of the magnetic moment can occur. To overcome this problem, we held the samples in long quartz tubes having an inner diameter slightly smaller than the largest dimension of the sample to be measured. The empty quartz tube extends through all three pickup coils of the magnetometer during a complete vertical scan of the magnetometer. It was verified that the tubes produced a negligible signal over the scan length used. For most of the SQUID measurements, the samples were inserted into the tubes with the maximum dimension parallel to the axis of the tube, then turned slightly to hold them in place. Care was taken to center the sample in the pickup coils at each temperature because of the displacement due to thermal contraction of the quartz tube.

When the measurements on the spherical sample were done, the above procedure was not possible and it was secured to the inside of the quartz tube with a small piece of Kapton tape. This mounting limited the measurements to a minimum field of about 0.5 mT. The second problem with low field

¹We are indebted to Larry Hulth and J. L. Smith of Los Alamos National Lab for annealing and x-raying this sample.

SQUID magnetometry is that the superconducting magnet retains trapped flux at low fields. The trapped flux can be removed partially by cycling between positive and negative fields with decreasing final fields. This was done at each temperature at which a measurement for H_{c1} was performed.

For temperatures between 2 and 32 K both constant temperature magnetic field hysteresis curves and constant field temperature hysteresis curves were recorded on two different crystals. At constant temperatures, measurements were taken as the field was raised from zero to a positive value greater than H_{c2} , then lowered through zero to a negative field value greater than H_{c2} . It was noted that any subsequent cycling of the field does not supply any additional information concerning the critical points. Hence, the symmetry of the complete hysteresis curves could be used to reduce the number of field points taken at a given temperature. An example of a complete constant temperature ($T = 22.5$ K) hysteresis curve is shown in Figure 1 with an expanded view showing H_r and H_{c2} in the inset. The temperature of the sample was raised to 50 K ($T > T_c$ at $H = 0$) before each constant temperature hysteresis measurement, then lowered to the measurement temperature in zero field. Thus, all constant temperature data reported are for zero field cooled samples. Samples not cooled in zero field would have a non-zero magnetization at zero field, but the magnetization curve for increasing field merges with the decreasing field portion at the same value of H_r .

Further measurements of H_{c2} and H_r were done using a cantilever force magnetometer at the National High Magnetic Field Laboratory (NHMFL) in a 27 T resistive magnet at temperatures from 1.4 to 19 K with the applied magnetic field being swept at a rate of 0.25 T/minute. The sample used for these measurements had a T_c of 30 K. An example of the constant temperature magnetic hysteresis curve taken with the force magnetometer is provided in Figure 2.

The constant field measurements were started at a temperature above T_c . The samples were cooled to 4.5 K in zero field, the field applied, the temperature slowly raised, point by point, to above T_c while recording magnetization, then again cooled to 4.5 K during the measurement in the applied field. An example of a complete cycle of this type of data is shown in Figure 3. Again, near T_c the magnetization is extremely small and care was taken to avoid the effects of the sample holder. Finally, we measured the magnetization at several temperatures at two constant fields in the normal state from 32 to 300 K to determine the normal state susceptibility.

4 Results

In addition to the separate H_{c1} measurements, there are several critical fields to be obtained from the hysteresis data: H_0 , H_{c2} , and H_r . The thermodynamic critical field H_0 is obtained only from the constant temperature data while H_{c2} and H_r were measured both at constant temperature and constant field. None of the critical fields can be determined in a straightforward manner and we state in detail how we have extracted them from the data. Between approximately 18 and 32 K, the two highest critical fields were determined using the SQUID magnetometer. Below 18 K, H_{c2} was in excess of the maximum field of the SQUID magnetometer (5.5 T). Above 22 K, H_{c1} was sufficiently low that no reliable data could be obtained.

4.1 H_{c1}

Values of H_{c1} reported here were obtained from the spherical sample from 4.2 to approximately 22 K. Typical low temperature, low field magnetization curves for several temperatures are shown in Figure 4. The initial slope of the curve is given by $M/H = V/4\pi (1-D)$, where V is the volume of the sample and D is the demagnetization factor. Only when the sample geometry is such that $D = 0$ will this constant slope extend to H_{c1} , at which point the magnetization would abruptly decrease. When $D \neq 0$, the field begins to penetrate the sample at different points gradually until the entire sample is in the mixed state. We shaped a single crystal sample into a sphere, ($D = 1/3$), hence the initial slope is much larger and the transition from the Meissner to the mixed state much sharper than for the crystals that have non-symmetric shapes.

To determine the value of H_{c1} , the following procedure was used. The low field, linear portion of the curve was fit with a straight line, and the field value at which the measured magnetization deviated from the straight line was taken to be $\frac{2}{3}H_{c1}$. Values obtained from this fit for H_{c1} are plotted as a function of temperature in Figure 5. Note that below 15 K these results give the same values as those reported in Grader et al. (1990).

4.2 H_0

The thermodynamic critical field is obtained by integrating over half the cycle, $M_R(H) = [M(H_{incr}) + M(H_{decr})]/2$, from zero to $> H_{c2}$. The value of

H_0 is obtained from:

$$\int M \cdot dH = \frac{H_0^2}{8\pi}. \quad (1)$$

Since SQUID magnetometry measurements require a constant applied field during the measurement, and the data were accumulated point by point we have numerically integrated the hysteresis curves to obtain H_0 at each temperature. The temperature dependence of H_0 is shown in Figure 6 for the sample used in the SQUID measurements. We have elected not to calculate values for H_0 from the high field-low temperature data until the anomalous “fishtail” structure (see below), also noticed by Gatalskaya et al. (1996), is fully understood. The fishtail adds area below the magnetization curve; thus, thwarting any attempt of straightforward analysis.

4.3 H_{c2}

A typical plot of the magnetization for increasing field from zero tesla to above H_{c2} is shown in Figure 1. There are several points about this curve that make determination of H_{c2} complicated. Between H_{c1} and H_{c2} the curve is never linear in applied field, and an extrapolation to H_{c2} from a linear portion of the curve in the superconducting state near H_{c2} is not possible (Hao, Clem, McElfresh, Civale, Malozemoff, and Holtzberg, 1991). Above H_{c2} BKBO is diamagnetic (mainly due to the atomic core contribution to the magnetization) and the total magnetization never becomes positive upon passing from the superconducting to the normal state. To obtain a consistent value for H_{c2} , we have fit the linear diamagnetism data in the normal state above H_{c2} to a straight line and taken the field at which the magnetization deviates from the extrapolation of this line to zero field to be H_{c2} . From values of H_{c2} obtained in this manner, we show the temperature dependence of H_{c2} in Figure 7 along with the determination of H_{c2} from the constant field data to be discussed below. The minimum in the magnetization curve in this field region is fairly broad for all of the samples, but this technique gives values of H_{c2} consistent with the ones that are obtained from temperature dependent data at constant field (Batlogg et al., 1988; Huang et al., 1991).

We observe the anomalous “fishtail” structure in our force magnetometer measurements also reported by Gatalskaya et al. (1996). These structures are not observed in the magnetization data taken with the SQUID magnetometer. This leads us to question the origin of these fishtails, specifically, whether they might be due to the measurement technique. The fishtails seen

in our force magnetometer measurements might be due to a magnetic field sweep rate that exceeds the flux lattice relaxation time, or may be associated with uncompensated torque contributions from the sample. It should be noted that these fishtail structures do not affect our ability to determine H_r and H_{c2} from these data, and these two critical fields are the only information we have extracted from the force measurements.

Using the 21 K values of H_{c1} and H_{c2} , the GL parameter, κ , was calculated from the relation

$$\frac{\ln \kappa}{2\kappa^2} = \frac{H_{c1}}{H_{c2}}. \quad (2)$$

We find that the value of κ at 21 K is approximately 64. This compares favorably with the value reported by Kwok, Welp, Crabtree, Vandervoort, Hulscher, Zheng, Dabrowski, and Hinks (1989) of $\kappa = 59$.

4.4 H_r

At temperatures above 15 K, we are able to determine the value of applied field at which the hysteretic behavior becomes reversible, H_r . We have taken this field to be the lowest value of H at which the increasing and decreasing applied field have the same measured values of M . The temperature dependence of H_r is shown in Figure 7.

4.5 Temperature Dependent Constant Field Data

Measurements of the temperature dependence of the magnetization at constant field give the same information in the T - H plane through measurements of critical temperatures, T_{c2} and T_r , as do the constant temperature field dependent measurements. A view of one set of data taken at constant field is shown in Figure 3. The temperature at which the magnetization deviates from a constant on the high temperature side is taken to be T_{c2} . The temperature at which the increasing and decreasing measurements deviate is T_r . One can see from the data presented in the inset of Figure 7 that the two different measurements give the same result. This agreement shows that the phase boundaries between the normal and superconducting states and between the reversible and irreversible flux regions within the superconducting states are equilibrium thermodynamic boundaries and are not controlled by non-equilibrium phenomenon.

4.6 Normal State Susceptibility

The normal state susceptibility, χ , was calculated from the difference of two magnetization curves taken at 0.3 T and 5.0 T at temperatures from 31 K to 350 K and is shown in Figure 8 with χ as a function of $1/T$ in the inset. The difference between the magnetization measurements, ΔM , divided by the field difference, ΔH , was taken to be the susceptibility, $\chi = \Delta M / \Delta H$. The reason for the large field difference for the two magnetization measurements is that M is small in each case, and the large ΔH reduces errors in ΔM . As long as the magnetization remains in the linear response regime, the relatively large size of ΔH is of no concern. The quartz tube sample holder contributes a small signal to the magnetization; this has been measured and subtracted from the difference magnetization.

5 Discussion

The temperature dependence and the magnitudes of the critical fields measured here are different from that expected from an ordinary type-II superconductor. In general, the critical fields have different temperature dependences from what is expected and some new phenomena are observed. We begin with a discussion of the normal state susceptibility.

In their initial measurements of the normal state susceptibility, Cava et al. (1988) found large extraneous paramagnetic contributions presumably due to the presence of unreacted KO_2 in their samples. In a following paper (Batlogg et al., 1988), the same authors corrected their data with an estimate of the core diamagnetism ($\chi_c \approx -7.5 \times 10^{-5}$ emu/mol) which is the same value used here. From their energy band calculations Mattheiss and Hamann (1988) determined the density of states at E_F in $\text{Ba}_{0.6}\text{K}_{0.4}\text{BiO}_3$ to be 0.46 states/eV. Using this value, we calculate the theoretical contribution to the susceptibility due to Pauli paramagnetism to be 2.7×10^{-5} emu/mol. Our measurements show that the normal state susceptibility at $T = 300$ K is -5.3×10^{-5} emu/mol (see Figure 8), and this value agrees with that reported by Hundley et al. (1989) and Uwe et al. (1996) for a potassium concentration of $x = 0.40$. Our measurements show an increase in the normal state paramagnetism below 150 K. We have fit the data below 150 K to a Curie-Weiss function plus a temperature independent Pauli term,

$$(\chi - \chi_{core}) = \chi_P + \frac{C}{T - \Theta}, \quad (3)$$

where χ_{core} is the core diamagnetism, χ_P is the Pauli term, C is the Curie constant, and Θ is the ordering temperature. The values obtained from the fits are $\chi_P = 1.81 \times 10^{-5}$ emu/mol, $C = 8.87 \times 10^{-4}$ erg K/G, and $\Theta = 2.48$ K for one sample and $\chi_P = 1.81 \times 10^{-5}$ emu/mol, $C = 8.28 \times 10^{-4}$ erg K/G, and $\Theta = 2.21$ K for a second sample. Using the values of C and assuming the impurities have a spin quantum number of $\frac{1}{2}$, the magnetic impurity concentration is estimated to be 0.66 % and 0.71 % for the two samples. If the impurities have a larger spin quantum number, then the magnetic impurity concentrations would be lower. The Pauli term for both samples is the same and is approximately 2/3 of that obtained from band theory (Mattheiss and Hamann, 1988). We point out that we have interpreted the linear $1/\chi$ vs. T behavior at low temperatures as being due to localized spin impurities. However, this behavior might also arise from other mechanisms intrinsic to the normal state.

If an overall linear fit to the H_{c1} data is done, a slope of $dH_{c1}/dT = -17.2 \pm 0.66$ G/K is obtained as compared to -11 G/K from Grader et al. (1990). These values are much larger than the value of Batlogg et al. (1988) of -4.5 ± 0.5 G/K; also, the values of H_{c1} derived from single crystals are larger than the powder samples used by Batlogg *et al.*. From this linear fit to the H_{c1} data, we find that $H_{c1}(T=0)$ is 393 ± 6 G. However, it is clear that a linear function does not represent best the H_{c1} dependence on temperature. Between 5 and 15 K the data appears to be linear. Around 15 K, $H_{c1}(T)$ experiences an inflection point and has a different curvature at higher temperatures. Attempts were made to measure H_{c1} at fields approaching T_c , but above 22 K the magnetization signal was too small to resolve with the SQUID measurement system near zero applied field.

We find that a good fit to the H_{c1} data above 12 K is obtained from $H_{c1}(T) \propto (1 - T/T_c)^3$ with the curve passing through the $H = 0$ value of $T_c = 29$ K. The very low value of H_{c1} is the reason the very broad temperature dependent magnetic transitions are observed in BKBO, even though the zero field resistive transitions are sharp. All of the magnetic measurements are made in small magnetic fields and continuous changes in $M(T)$ are observed until the temperature is reached where H_{c1} is greater than the measurement field. We note that H_{c1} is the only measured thermodynamic critical field that does not have upward curvature as the temperature goes to zero.

As a result of our upper critical field measurements, we found that a power law fit where H_{c2} and $H_r \sim (1 - T/T_c)^m$ yielded values of $m = 1.58$ and 1.97 for H_{c2} and H_r respectively (as shown in Figure 9). Gatalskaya

et al. (1996) found for H_r that $m = 1.45$ for a sample with a potassium concentration of 0.34. Also, Goll et al. (1996) report a value of $m = 1.5$ for H_r in their below optimum potassium concentration sample. Our samples had a nominal potassium concentration of 0.40.

Welp et al. (1988) report upper critical field slopes for several concentrations of K, but no positive curvature of the H_{c2} versus temperature was reported. Like Affronte et al. (1994) and Gantmakher et al. (1996), we observe a positive curvature in the H_{c2} versus temperature curve; however, we observe an enhanced curvature as compared to the results of Gantmakher et al. (1996). This curvature deviates significantly from the universal behavior predicted by Werthamer, Helfand, and Hohenberg (WHH) (Werthamer, Helfand, and Hohenberg, 1966) for superconductors with weak electron-phonon coupling. Gantmakher et al. (1996) find empirically that their H_{c2} data fits the function

$$H_{c2}(T) = 32.2 - 1.8 T + 0.025 T^2. \quad (4)$$

A plot of this equation is shown in Figure 7. Our H_{c2} data show a greater curvature than the fit of Gantmakher et al. (1996) and it appears a second order fit greatly underestimates the probable value of $H_{c2}(T=0)$, and their value of 32.2 T might be too low. Gantmakher et al. (1996) comment that the positive curvature is enhanced by disorder in the sample; therefore, the enhancement of the curvature and correspondingly in $H_{c2}(T=0)$ may be due to an intrinsic disorder in BKBO.

From our determination of H_r we observe that the irreversibility line also deviates from WHH theory and displays a positive curvature. Similarly, Goll et al. (1996) observe a positive curvature in H_r versus temperature, and again our values of H_r are enhanced when compared with the values of Goll et al. (1996). Similarly, the thermodynamic critical field, H_0 , has a positive curvature as is shown in Figure 6.

Samuely et al. (1996) have determined the upper critical field H_{c2} by Andreev reflection in point-contact junctions, a measurement of the superconducting density of states. They find no positive curvature of the H_{c2} versus temperature curve and claim that their measurements confirm an adherence of BKBO to WHH theory. This contradicts all other magneto-transport measurements (Affronte, Marcus, Escribe-Filippini, Sulpice, Rakoto, Broto, Ousset, Askenazy, and Jansen, 1994) that uniformly show H_{c2} and H_r as a function of temperature in BKBO deviate from WHH theory. The only remarkable difference between the samples used by Samuely et al. (1996) and

other groups is that their samples had a T_c of ≈ 23 K. Studies, including this one, that use samples with T_c s of 30 to 32 K generally show a deviation from the WHH theory.

Measurement of magnetization across a phase transition may contain fluctuation effects. Following early works of Aslamazov and Larkin (1968), Ullah and Dorsey (1991) have proposed a scaling equation for temperature and field dependence of magnetization. The scaling variables used are

$$\begin{aligned} [T - T_c(H)] / [HT]^{2/3} & \quad D = 3 \\ [T - T_c(H)] / [HT]^{1/2} & \quad D = 2 \end{aligned} \quad (5)$$

where the dimensionality of the electron system is given by D . For either $D=3$ or $D=2$ the magnetization is expected to follow a universal curve. The essential feature is that a smooth cross over takes place from a normal paramagnetic (or diamagnetic in the case of BKBO) state to the mixed state of a superconductor. Thermodynamic quantities such as the magnetization and specific heat for YBCO have been shown to fit a 3D universal curve by Welp et al. (1991) The results of our H_{c2} data being analyzed in this manner are shown in Figure 10. One can see that the data for magnetization collapse onto a universal curve. However, given that BKBO is a cubic isotropic system, it is surprising that our results are just as well described by $D=2$ or $D=3$. It appears that fluctuation theory cannot distinguish between 2 and 3 dimensional behavior in this case. Therefore, the broadening of the transition may be due to effects other than fluctuations.

Several studies of the specific heat of BKBO have been done (Hundley, Thompson, and Kwei, 1989; Graebner, Scheenmeyer, and Thomas, 1989; Stupp, Reeves, Ginsberg, Hinks, Dabrowski, and Vandervoort, 1989; Alba, 1992). All but one study (Graebner et al., 1989) conclude that ΔC_p is zero across the transition. Because of the large phonon contribution to the specific heat and the low density of electronic states, it is difficult to extract the comparatively small value of the electronic specific heat change across the transition. A calculation by Kwok et al. (1989) shows the BCS discontinuity in BKBO to be $\Delta C_p / T_c \approx 3.75$ mJ/mole K^2 or $\Delta C_p = 120$ mJ/mole K if $T_c = 32$ K. This value is calculated from the relation

$$\Delta C_p / T_c = \left(\frac{1}{8\pi\kappa^2} \right) \left(\frac{dH_{c2}}{dT} \right)^2, \quad (6)$$

where $\kappa \simeq 64$ is the Ginzburg-Landau parameter at low temperatures. At temperatures near T_c , the magnitude of the total specific heat is in the range

of 15 to 20 J/mole K, and the expected discontinuity is approximately 0.1 J/mole K. Previous measurements of the specific heat performed at LSU (chun Xu and Goodrich, 1989) using a sensitive ac technique (chun Xu, Watson, and Goodrich, 1990) did not detect a discontinuity in C_p at the transition temperature and we believe the measurements were of sufficient accuracy to detect a ΔC_p of the order of magnitude predicted by Kwok et al. (1989). Recently, more high sensitivity measurements have been performed by Kim and Stewart ² Again no discontinuity in C_p is observed.

If one observes a second order phase transition as the normal-superconducting (N-S) phase boundary is crossed, a signature of the transition can be obtained from the temperature dependence of the thermodynamic critical field. In a second order phase transition, the free energy $F = H_0^2/8\pi \propto (1 - T/T_c)^2$. Thus, $H_0(T)$ is expected to be linear in $(1 - T/T_c)$. In Figure 6, the measured temperature dependence of the thermodynamic critical field H_0 is given with the fit to $(1 - T/T_c)^2$ shown in the inset. This result clearly shows that the usual second order phase theory does not fit the data.

The experimental results for critical fields H_{c1} , H_r , and H_{c2} also are different from conventional superconductors in detail. More specifically, they are anomalous in subtle but important ways.

First, the GL parameter κ as seen from equation 2 is temperature dependent (see Figure 11). In a BCS-GL framework (Tinkham, 1980), $\kappa (= \lambda/\xi)$ is temperature independent near T_c . Indeed the entire classification of superconductivity between types I and II rests on a constant κ (whether $< 1/\sqrt{2}$ or not).

We see here that $H_{c1} \propto (1 - T/T_c)^3$ and $H_{c2} \propto (1 - T/T_c)^{3/2}$, leading to $\kappa \propto (1 - T/T_c)^{-3/4}$ using equation 2. The divergence of κ near T_c indicates a much softer Meissner effect than seen in conventional superconductors.

Next, the principal premise of BCS-GL theory is a second order phase transition. The Ehrenfest relation for this second order phase transition is given by

$$\left(\frac{dH_{c2}}{dT}\right)^2 = \frac{\Delta C}{T_c \Delta \chi}, \quad (7)$$

where ΔC is the discontinuity in the specific heat and $\Delta \chi$ is the discontinuity in the magnetic susceptibility. As stated above, there is evidence that $\Delta C = 0$. In our measurements, we find $\Delta \chi = 0$.

²J. Kim and G. Stewart, University of Florida, Private Communication.

It is worth noting that BKBO, a diamagnet, is a propitious superconductor to look for non-BCS-GL effects. In a conventional superconductor, in the mixed state, the magnetic response is diamagnetic, although the magnetic susceptibility ($\frac{\partial M}{\partial H}$) is positive, since M is negative. However, in the normal state most metals are weakly paramagnetic. Thus when the transition from a superconductor to a normal metal occurs, $\Delta M \neq 0$ and the transition is weakly first order. In BKBO, there is no discontinuity in M ; the magnetization smoothly connects to the diamagnetism of the normal state. Since both ΔM and $\Delta \chi$ appear to be zero, the order of the phase transition could be higher than two. We point out that an indication of the transition order can be obtained from the thermodynamic critical field H_0 . In a phase transition of order n , $F = \frac{H_0^2}{8\pi} \propto (1 - T/T_c)^n$. Thus the fit shown in Figure 6 suggests a fourth order phase transition where $H_0 \propto (1 - T/T_c)^2$.

If the transition is indeed higher than second order in the Ehrenfest sense, then, the temperature dependence of specific heat will not show a discontinuity at T_c . There should be a discontinuity in the derivatives of the specific heat; however, a measurement near T_c will show effectively no sharp change in C .

In a previous paper (Kumar, 1997), the properties of a third order phase transition have been developed. When these same arguments are extended to a fourth order phase transition (Kumar et al., 1999) with a free energy F_{IV} the temperature dependance of H_{c1} and H_{c2} can be calculated from the free energy F_{IV} and the length scale $\xi^2 \sim c/a \sim (1 - T/T_c)^{-1}$ yielding $H_{c2} = \Phi_0/2\pi\xi^2 \propto (1 - T/T_c)$. The exponent is obtained in a mean field analysis and is lower than the observed exponent of 1.5 (1.25 near T_c , see Fig. 9 caption). However, as pointed out by Gantmakher et al. (1996) the curvature in H_{c2} can be enhanced by sample disorder. Next, the temperature dependence of $H_{c1} \sim \phi_0/\lambda^2 \propto (1 - T/T_c)^3$. This is in agreement with the experiment; as is the corresponding $\kappa = \lambda/\xi$ in its temperature dependence.

Our conclusions about the possible order of the SC transition are published in Kumar et al. (1999); however much work still needs to be done to properly understand the nature of inhomogeneities and the effects they have on the critical magnetic fields. In addition, further analysis of fluctuations needs to be done. Thus, whether macroscopic fluctuations can lead to a different temperature dependance of the irreversibility field H_r which can influence the calculated values of H_0 also remains to be analyzed.

6 Conclusions

Our magnetization measurements have been carried out as field dependence at constant temperature and temperature dependence at constant field to determine the critical fields for BKBO. In all cases the agreement between the results of these two independent measurements indicate that we are measuring equilibrium properties.

From high temperature (31 - 350 K) susceptibility measurements we determine the conduction electron Pauli susceptibility to be 1.8×10^{-5} emu/mol for two samples. The total susceptibility also contains an ostensible ferromagnetic term with a Curie-Weiss temperature near 2 K.

We report results of the first force magnetometer measurements of BKBO to fields up to 27 T, and show that the H_{c2} and H_r critical field curves deviate from WHH theory (Werthamer et al., 1966), displaying a positive curvature at low temperatures. Our overall results including both force and SQUID measurements for these two critical fields are in general agreement with previous measurements, but show higher values of H_{c2} and H_r at low temperatures than previously have been reported. We find that while fluctuation scaling theory fits the data from the SQUID measurements near H_{c2} , no distinction can be made between two or three dimensional theory. This result indicates that fluctuations may not be the cause of the broadness of the transition.

Finally, we note that BKBO may exhibit a phase transition that is not of thermodynamic order two. The conclusion that the order is higher than two is based on previous measurements of the specific heat in the normal and superconducting state across the transition (no observed discontinuity), on measurements of the susceptibility across the transition (no $\Delta\chi$), and on the fact that BKBO is a normal state diamagnet. The temperature dependence of the thermodynamic critical field (near T_c), has led us to suggest that the transition is of order four. (Kumar et al., 1999) Furthermore, this is consistent with the experimental temperature dependence of H_{c1} and is close to the temperature dependence of H_{c2} . We note that near T_c , the Ginzburg-Landau parameter, $\kappa = \frac{\lambda}{\xi}$, is temperature dependent, $\kappa \sim (1 - T/T_c)^{-3/4}$, a divergence which points to an unusually soft Meissner effect at T_c .

Perhaps the most significant difficulty in analysis of the present data (and the data in earlier references on thermodynamic properties of BKBO) is that one's intuition is based on a tacit assumption that all superconducting transitions are second order with associated fluctuation effects. The expected properties of higher order phase transitions are different yet one tries to un-

derstand an anomalous property in terms which implicitly assume a second order phase transition. However, the evidence presented here for a higher order phase transition is by no means conclusive.

The experimental data presented here is (1) largely consistent with earlier efforts on samples of similar quality and (2) where the results are new, there may be a formalism, based on a higher order phase transition that may explain the known anomalies.

7 Acknowledgments

The work at LSU was supported by the NSF under grant No. DMR-9501419. A portion of this work was performed at the National High Magnetic Field Laboratory, which is supported by NSF Cooperative Agreement No. DMR-9016241 and by the State of Florida. The Norton group effort was supported by the NSF under grant No. CHE-9612568.

References

- M. Affronte, J. Marcus, C. Escribe-Filippini, A. Sulpice, H. Rakoto, J. M. Broto, J. C. Ousset, S. Askenazy, and A. G. M. Jansen. Upper critical field of $\text{Ba}_{1-x}\text{KxBiO}_3$ single crystals. *Phys. Rev. B*, 49(5):3502–3510, 1994.
- Eduardo Alba. Automated adiabatic calorimetry, and the specific heat of $\text{Ba}_{1-x}\text{KBiO}_3$. Master’s thesis, Louisiana State University, 1992.
- Aslamazov and Larkin. *Phys. Lett.*, 26A:238, 1968.
- B. Batlogg. Superconductivity in $\text{Ba}(\text{Pb}, \text{Bi})\text{O}_3$. *Physica B*, 126:275, 1984.
- B. Batlogg, R. J. Cava, L. W. Rupp, A. M. Mujsce, J. J. Krajewski, J. P. Remika, W. F. Peck, A. S. a. Cooper, and G. P. Espinosa. Density of states and isotope effect in BiO superconductors: Evidence for nonphonon mechanism. *Phys. Rev. Lett.*, 61:1670, 1988.
- J. G. Bednorz and K. A. Müller. Possible high T_c superconductivity in the Ba-La-Cu-O system. *Z. Phys. B*, 64:186, 1986.
- R. J. Cava, B. Batlogg, J. J. Krajewski, R. Farrow, Jr, L. W. Rupp A. E. White, K. Short, W. F. Peck, and T. Kometani. Superconductivity near

- 30 K without copper: the $\text{Ba}_{0.6}\text{K}_{0.4}\text{BiO}_3$ pervoskite. *Nature*, 332:814, 1988.
- Jing chun Xu and R. G. Goodrich. 1989.
- Jing chun Xu, C. H. Watson, and R. G. Goodrich. A method for measuring the specific heat of small samples. *Rev. Sci. Inst.*, 61(2):814, 1990.
- B. Dabrowski, D. G. Hinks, J. D. Jorgensen, R. K. Kalia, P. Vashishta, D. R. Richards, D. T. a. Mark, and A. W. Mitchell. Variable-range hopping conduction in $\text{Ba}_{1-x}\text{K}_x\text{BiO}_3$ -y system. *Physica C*, 152:24, 1988.
- V. F. Gantmakher, L. A. Klinkova, N. V. Barkovskii, G. E. Tsydynzhapov, S. Wieggers, and A. K. Geim. Positive curvature in the temperature dependence of H_{c2} in $\text{KxBa}_{1-x}\text{BiO}_3$. *Phys. Rev. B*, 54(9):6133–6136, Sept 1996.
- Valentina I. Gatal'skaya, Sergei N. Barilo, Sergei V. Shirayev, Henrick Szymezak, Rita Szymezak, and Marek Baran. Study of magnetic irreversibility line of BKBiO single crystals near T_c . *Czechoslovak J. of Phys.*, 46:845, 1996.
- G. Goll, A. G. M. Jansen, and J. Marcus. Temperature dependence of the irreversibility field of $\text{Ba}_{1-x}\text{K}_x\text{BiO}_3$. *Czechoslovak J. of Phys.*, 46(Suppl. S2):849, 1996.
- G. S. Grader, A. F. Hebard, and L. F. Scheenmeyer. Magnetization measurements of $5\text{ }\mu\text{m}$ $\text{Ba}_{0.6}\text{K}_{0.4}\text{BiO}_3$ crystals: Approach to intrinsic behavior with decreasing size. In David Christen, Jadish Narayan, and Lynn Schneemeyer, editors, *High-Temperature Superconductors: Fundamental Properties and Novel Materials Processing*, volume 169 of *Materials Research Society Symposium Proceedings*, pages 1081 – 1084, Pittsburgh, Pennsylvania, 1990. Materials Research Society.
- J. E. Graebner, L. F. Scheenmeyer, and J. K. Thomas. Heat capacity of superconducting $\text{Ba}_{0.6}\text{K}_{0.4}\text{BiO}_3$ near T_c . *Phys. Rev. B*, 39(13):9682 – 9684, 1989.
- Z. Hao, John R. Clem, M. W. McElfresh, L. Civale, A. P. Malozemoff, and F. Holtzberg. Model for the reversible magnetization of high- κ type-II superconductors. *Phys. Rev. B*, 43:2844, 1991.

- D. G. Hinks, B. Dabrowski, J. D. Jorgensen, A. W. Mitchell, D. R. Richards, S. Pei, and D. Shi. Synthesis, structure and superconductivity in the $\text{Ba}_{1-x}\text{K}_x\text{BiO}_3$ system. *Nature*, 333:836, 1988.
- Z. J. Huang, H. H. Fang, Y. Y. Xue, P. H. Hor, C. W. Chu, M. L. Norton, and H. Y. Tang. Study of the magnetic properties of single-crystal $\text{Ba}_{0.6}\text{K}_{0.4}\text{BiO}_3$. *Physica C*, 180:331 – 336, 1991.
- M. F. Hundley, J. D. Thompson, and G. H. Kwei. Specific heat of the cubic high-Tc superconductor $\text{Ba}_{0.6}\text{K}_{0.4}\text{BiO}_3$. *Solid State Commun.*, 70:1155 – 1158, 1989.
- R. Itti, I. Tomeno, K. Ikeda, K. Tai, N. Koshizuka, and S. Tanaka. Photoelectron spectroscopic study of $\text{Ba}_{1-x}\text{Rb}_x\text{BiO}_3$. *Phys. Rev. B*, 43:435, 1991.
- Pradeep Kumar. Properties of phase transitions of a higher order. *J. Low Temp. Phys.*, 106(5/6):705–716, 1997.
- Pradeep Kumar, Donavan Hall, and R. G. Goodrich. Thermodynamics of the superconducting phase transition of $\text{Ba}_{0.6}\text{K}_{0.4}\text{BiO}_3$. *Phys. Rev. Lett.*, 82(22):4532, May 1999.
- W. K. Kwok, U. Welp, G. W. Crabtree, K. G. Vandervoort, R. Hulscher, Y. Zheng, B. Dabrowski, and D. G. Hinks. Magnetic and resistive measurements of the superconducting critical fields of melt-cast $\text{Ba}_{0.65}\text{K}_{0.35}\text{BiO}_3$. *Phys. Rev. B*, 40(13):9400–9403, 1989.
- L. F. Mattheiss, E. M. Gyorgy, and D. W. Johnson Jr. Superconductivity above 20 K in the Ba-K-Bi-O system. *Phys. Rev. B*, 37(7):3745 – 3746, 1988.
- L. F. Mattheiss and D. R. Hamann. Electronic structure of the high-Tc superconductor $\text{Ba}_{1-x}\text{K}_x\text{BiO}_3$. *Phys. Rev. Lett.*, 60:2681, 1988.
- M. E. McHenry, P. M. Maley, G. H. Kwei, and J. D. Thompson. Flux creep in a polycrystalline $\text{Ba}_{0.6}\text{K}_{0.4}\text{BiO}_3$. *Phys. Rev. B*, 39:7339, 1989.
- M. L. Norton and H-Y. Tang. *Chem. Mater.*, 3:431–434, 1991.

- P. Samuely, P. Szabo, A. G. M. Jansen, P. Wyder, J. Marcus, L. Baril, and C. Escribe-Filippini. Upper critical magnetic field in the superconducting bismuthates studied by the point-contact spectroscopy. *Czechoslovak J. of Phys.*, 46(Suppl. S2):847, 1996.
- H. Sato, S. Tajima, H. Takagi, and S. Uchida. Optical study of the metal-insulator transition on $\text{Ba}_{1-x}\text{K}_x\text{BiO}_3$ thin films. *Nature*, 338:241, 1989.
- A. W. Sleight, J. L. Gilson, and P. B. Bierstedt. *Solid State Commun.*, 17:27, 1975.
- S. E. Stupp, M. E. Reeves, D. M. Ginsberg, D. G. Hinks, B. Dabrowski, and K. G. Vandervoort. Low-temperature specific heat of polycrystalline $\text{Ba}_{0.6}\text{K}_{0.4}\text{BiO}_3$. *Phys. Rev. B*, 40(10):10878 – 10881, 1989.
- Michael Tinkham. *Introduction to Superconductivity*. Robert E. Krieger Publishing Company, Malabar, Florida, 2nd. edition, 1980.
- Ullah and Dorsey. *Phys. Rev. B*, 44:262, 1991.
- Hiromoto Uwe, Xiaoli Ji, and Hidetoshi Minami. Magnetic susceptibility of single crystalline $\text{Ba}_{1-x}\text{K}_x\text{BiO}_3$. *Czechoslovak J. of Phys.*, 46(Suppl. S5):2691, 1996.
- U. Welp, S. Fleshler, W. K. Kwok, R. A. Klemm, V. M. Vinokur, J. Downey, B. Veal, and G. W. Crabtree. High-field scaling behavior of thermodynamic and transport quantities of $\text{YBa}_2\text{Cu}_3\text{O}_{7-\delta}$ near the superconducting transition. *Phys. Rev. Lett.*, 67(22):3180–3183, November 1991.
- U. Welp, W. K. Kwok, G. W. Crabtree, H. Claus, K. G. Vandervoort, B. Dabrowski, A. W. Mitchell, D. R. Richards, D. T. Marx, and D. G. Hinks. The upper critical field of $\text{Ba}_{1-x}\text{K}_x\text{BiO}_3$. *Physica C*, 156:27, 1988.
- N. R. Werthamer, E. Helfand, and P. C. Hohenberg. Temperature and purity dependence of the superconducting critical field, H_{c2} . III Electron spin and spin-orbit effects. *Phys. Rev.*, 147(1):295, 1966.

FIGURE CAPTIONS

Figure 1. Complete hysteresis curve taken at 22.5 K from $H = 0$ to 5.5 T, back through zero to - 5.5 T and then to > 0 . An expanded view of the data showing H_r and H_{c2} is given in the inset.

Figure 2. Hysteresis in the magnetization as a function of applied field of $\text{Ba}_{0.6}\text{K}_{0.4}\text{BiO}_3$ at 6.0 K from zero to $> +H_{c2}$ to zero. This data is the magnetization determined from the force magnetometer. H_r is indicated. The arrows show the direction of the field sweep. Note that as H goes to zero, the field gradient, and therefore, the force also goes to zero.

Figure 3. Example of a magnetization hysteresis taken at constant field ($H = 50000$ G).

Figure 4. Magnetization as a function of applied field for the spherical sample of $\text{Ba}_{0.6}\text{K}_{0.4}\text{BiO}_3$ at a number of temperatures. The temperatures from from 5 K for the highest curve to 17.5 K for the lowest.

Figure 5. Values of H_{c1} of $\text{Ba}_{0.6}\text{K}_{0.4}\text{BiO}_3$ as a function of temperature determined from magnetization data on the spherical sample. The inset shows that H_{c1} goes as $(1 - T/T_c)^3$ for temperatures higher than 12 K.

Figure 6. Values of the thermodynamic critical field for BKBO obtained from integration of the magnetic hysteresis curves as a function of temperature. The inset shows that in the fit $(1 - T/T_c)^{n/2}$ that $n = 4$, thereby showing that the superconducting transition is of order 4.

Figure 7. Values of H_{c2} measured as a function of temperature for BKBO are shown along with the values of H_r and H_{c2} . H_{c2} values from both constant field and constant temperature measurements are represented by a \square while H_{c2} values for the sample used in the force magnetometer measurements, are represented by a \diamond . The arrow indicates that at temperatures below 10 K H_{c2} exceeded fields of 27 tesla, and H_r values from both constant field and constant temperature measurements are represented by a \triangle . The H_r values from the force measurements are represented by a \bowtie . The dotted line is the phenomenological fit to other data given by Gantmakher *et al.* (Gantmakher *et al.*, 1996). The inset shows the measured values of H_{c2} (\circ), T_{c2} (\otimes), H_r (\diamond), and T_r (\square) as a function of temperature.

Figure 8. The normal state susceptibility as a function of temperature for two $\text{Ba}_{0.6}\text{K}_{0.4}\text{BiO}_3$ samples. The inset shows that χ is linear in $1/T$ for

low temperatures. The lines are a guide to the eye.

Figure 9. Temperature dependence of H_{c2} and H_r from the force magnetometer and SQUID measurements combined. Note that if only the high temperature SQUID data is used, the critical exponent drops to 1.25 for H_{c2} .

Figure 10. 3D scaling of the magnetization data near T_c . 2D scaling is shown in the insert.

Figure 11. The Ginzburg-Landau parameter, $\kappa = \frac{\lambda}{\xi}$, calculated from values of H_{c1} and H_{c2} at selected temperatures as a function of temperature.

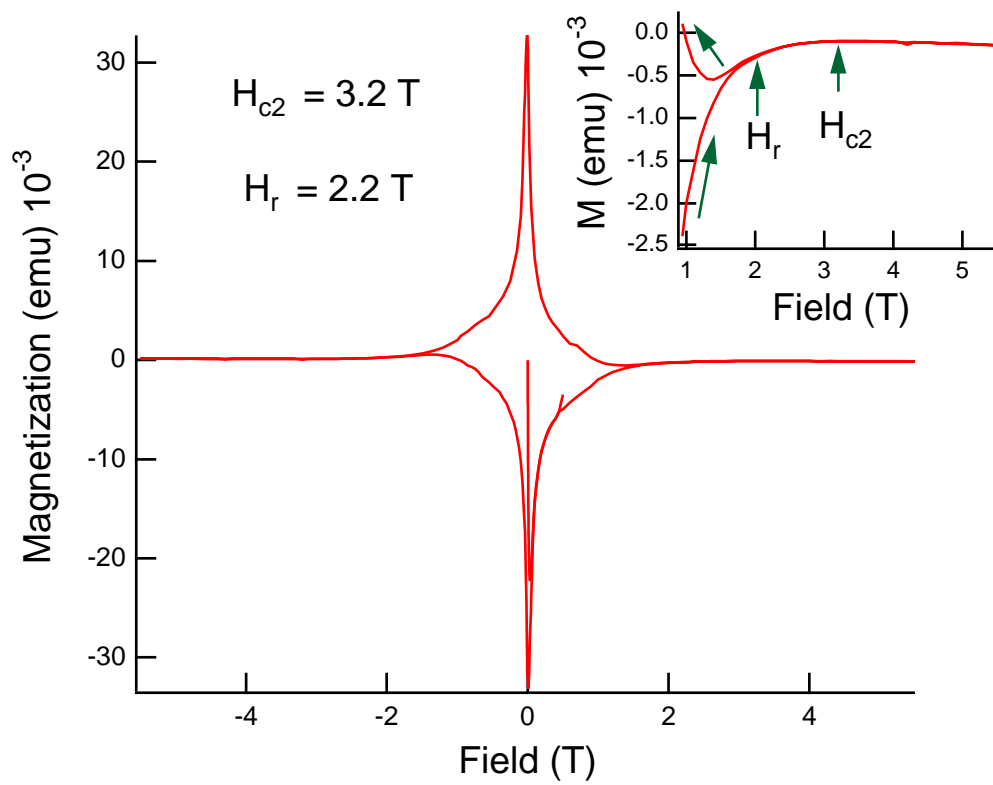


Figure 1:

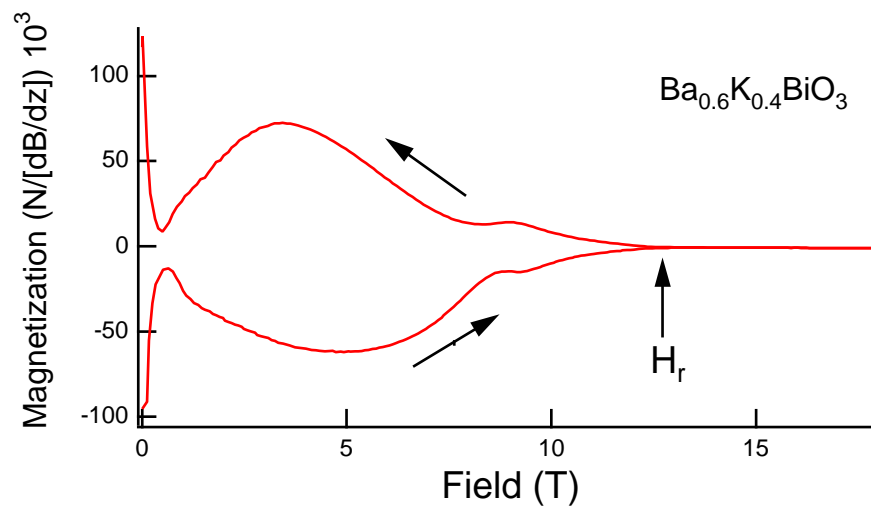


Figure 2:

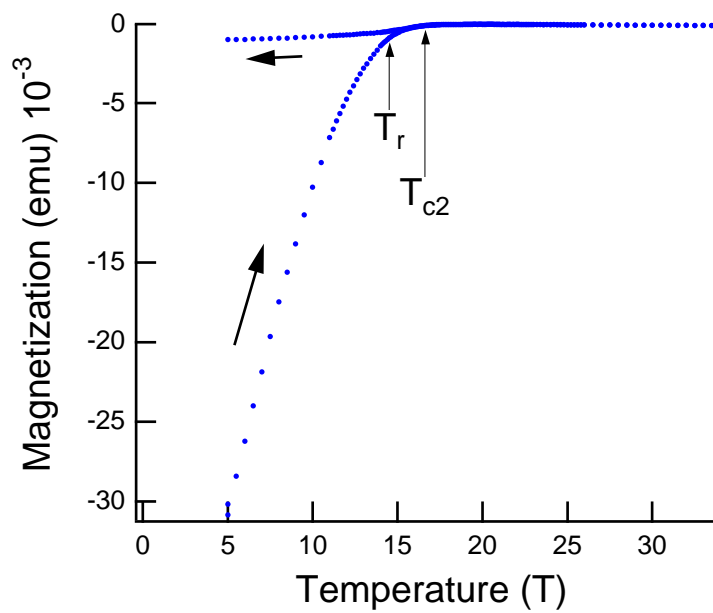


Figure 3:

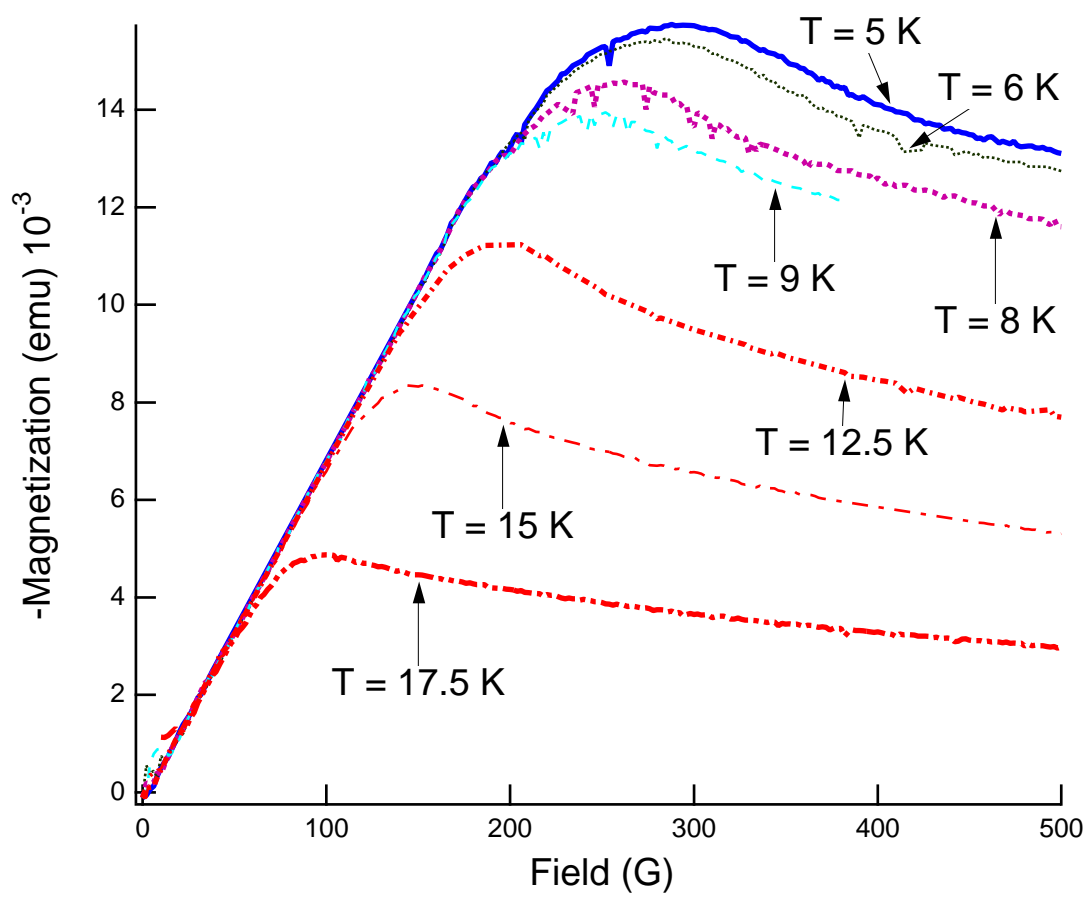


Figure 4:

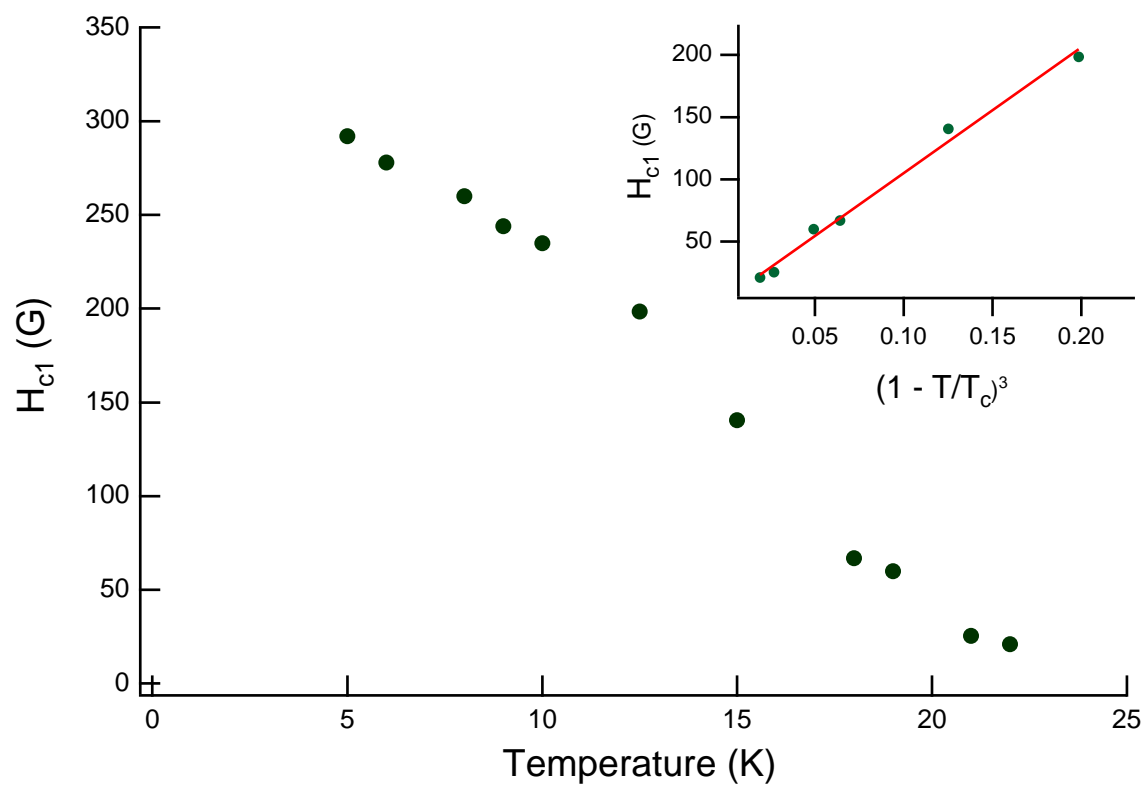


Figure 5:

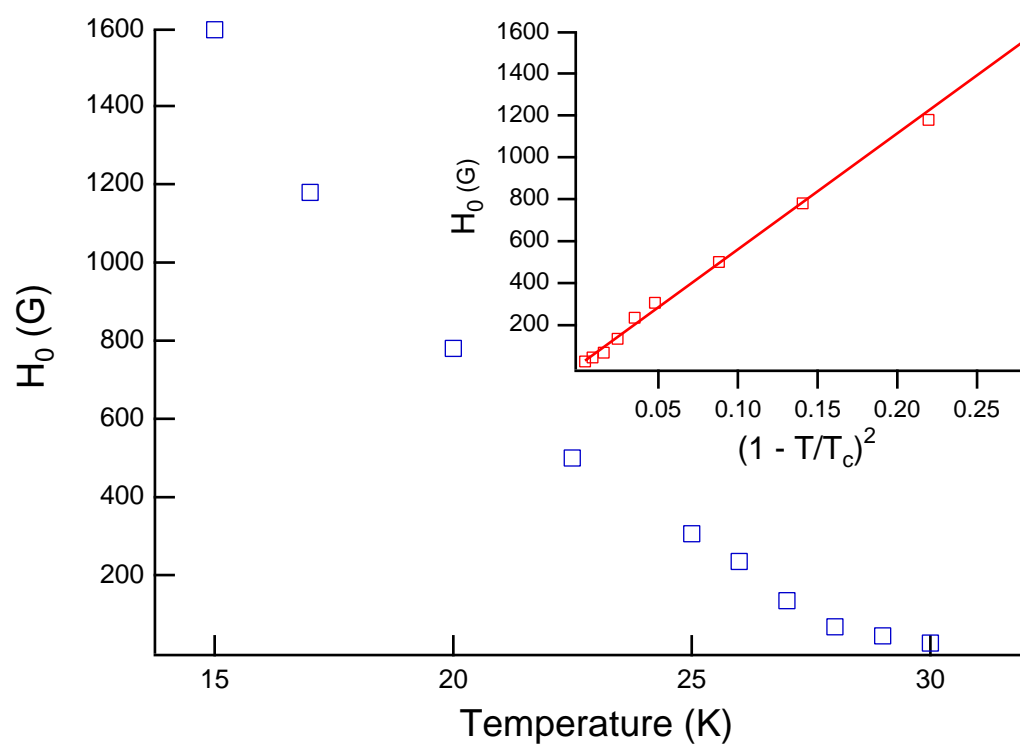


Figure 6:

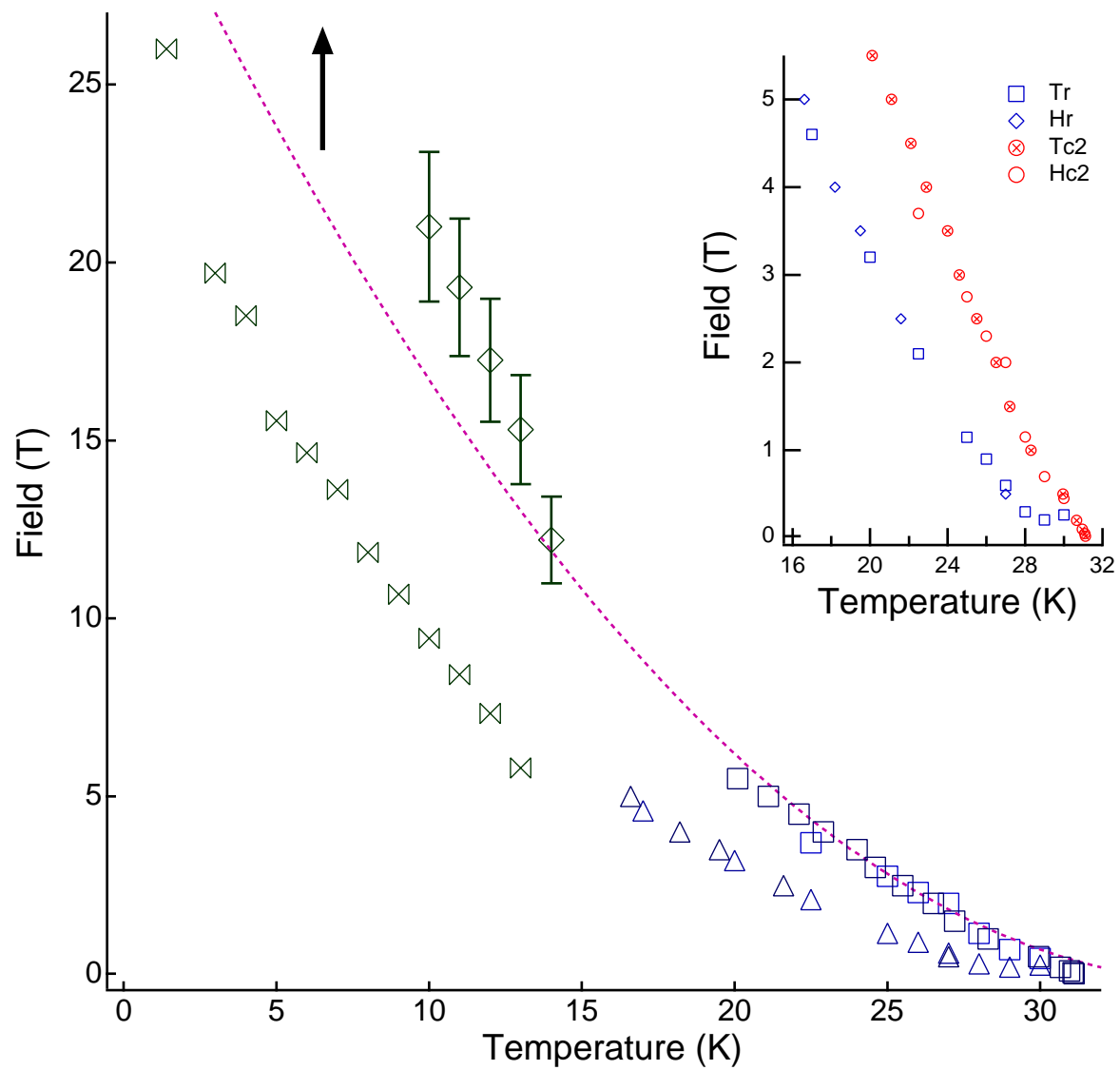


Figure 7:

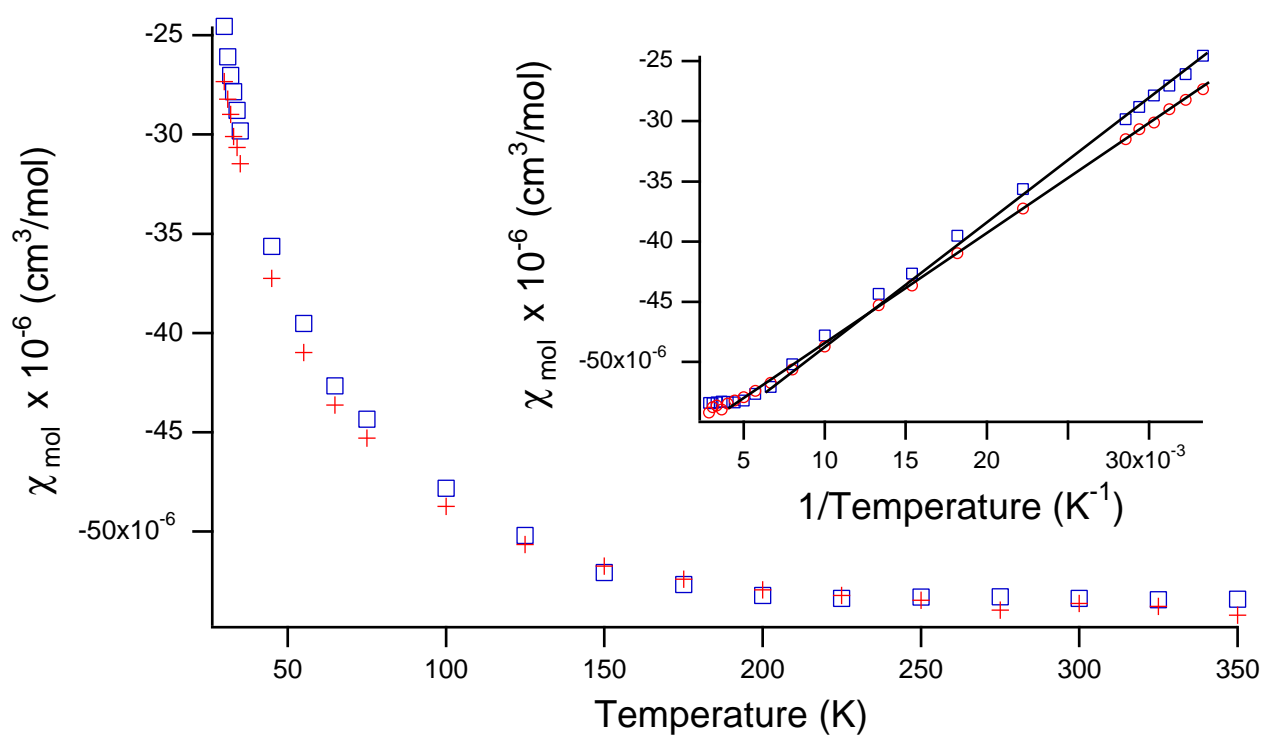


Figure 8:

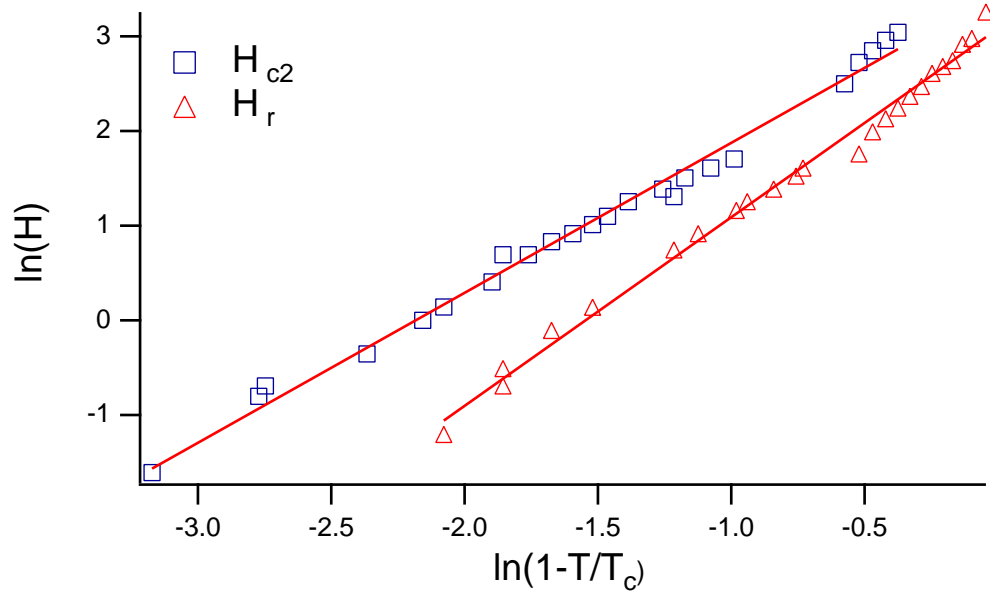


Figure 9:

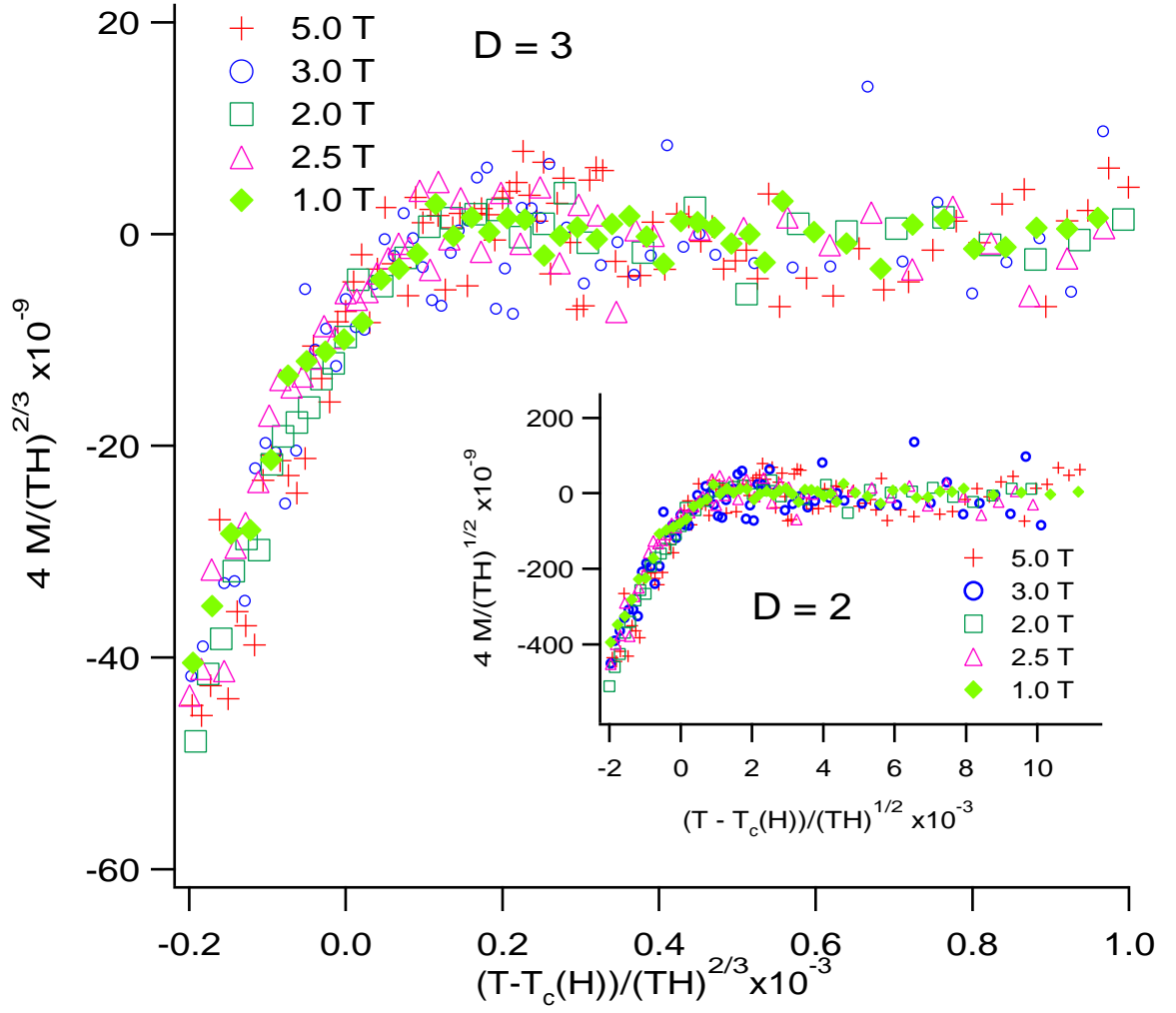


Figure 10:

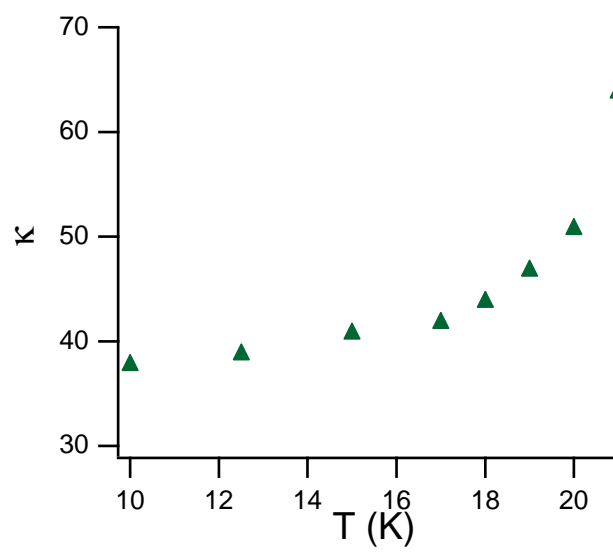


Figure 11: